PROBABILISTIC INFERENCE METHOD TO DISCRIMINATE CLOSED WATER FROM SEA ICE USING SENTINEL-1 SAR SIGNATURES

Christoph Herbert, Adriano Camps and Mercè Vall-llossera

CommSensLab, Universitat Politècnica de Catalunya (UPC) and
Institut d'Estudis Espacials de Catalunya (IEEC/CTE-UPC), Barcelona, Spain

ABSTRACT

Consistent sea ice monitoring requires accurate estimates of sea ice concentration. Current retrieval algorithms are based on low-resolution microwave radiometry data with limited penetration depth and are unable to resolve surface characteristics of sea ice in sufficient detail which is necessary to discriminate intact sea ice from closed water. Important information about surface roughness conditions are contained in the distribution of radar backscattering images which can be - in principle - used to detect melt ponds and different sea ice types. In this work, a two-step probabilistic approach based on Expectation-Maximization and Bayesian inference considers the spatial and statistical characteristics of medium-resolution daily-available Sentinel-1 SAR images. The presented method segments sea ice into a number of separable classes and enables to discriminate surface water from the remaining sea ice types.

***Index Terms*—** Bayesian Inference, Sentinel-1 Synthetic Aperture Radar (SAR), sea ice, melt ponds

1. INTRODUCTION

Sea ice concentration (SIC) is defined as the fraction of an observed area covered by sea ice. Satellite-based maps of SIC have been generated since 1979 starting with the launch of the Scanning Multichannel Microwave Radiometer (SMMR) and follow-on missions [1]. The penetration depth of microwave radiometers into ice at frequencies above 5 GHz is in the order of mm and water on top of the ice cannot be distinguished from sea water. Thus, current SIC estimates exclusively reflect the two-dimensional surface and leave out necessary information about sea ice conditions, which are in turn directly related to the surface. Especially in Arctic summer, sea ice is considered a heterogeneous medium consisting of various surface structures such as melt ponds and slushes composed of wet snow and sea ice. Melt ponds occur among multiple scales, are difficult to detect from low-resolution images, and a melt pond cycle from its origin to re-freeze up can be divided into discrete stages [2]. A more specified distinction between fractions of intact sea ice, melt ponds, and closed sea water is required to eliminate ambiguities in models and retrieval algorithms which are build upon these estimates.

Several methods have been developed to detect melt ponds based on air- and spaceborne observations among different scales using microwave radiometry, radar and optical data [3, 4, 5]. This study presents a probabilistic approach to discriminate sea ice from surface water using Sentinel-1A/B Synthetic Aperture Radar (SAR) images, which are available on a daily basis at medium resolution (~40 m) covering the entire polar area. The intensity of radar backscattering is sensitive to the surface roughness. Surface roughness for closed water and sea ice is significantly smaller as compared to the mainly wind-forced open ocean, which enables to classify surface types based on its intrinsic surface conditions. The goal is to segment SAR images into a number of separable classes using a two-step method, combining an Expectation-Maximization (EM) step with Bayesian inference modeling based on Gaussian Mixture Models (GMM). The approach considers the angular variations and the spatial correlations of the SAR images. This work focuses on the methodology and presents preliminary estimates of surface water fraction based on annual images at a selected area in the Northern Barents Sea from September 1, 2019 to August 31, 2020.

2. DATA AND STUDY AREA

The Sentinel-1 mission - developed by the European Space Agency (ESA) for the European Commission - was launched in April 2014 and is composed of two polar-orbiting satellites, Sentinel-1A and Sentinel-1B, providing dual polarisation capability, very short revisit times and rapid product delivery [6]. The SAR operates at C-band (5.405 GHz) and data are collected in ascending and descending orbit direction independent of daylight under all weather conditions, with an incidence angle ranging from 18.3 $^\circ$ to 46.8 $^\circ$. Data over sea and polar areas are acquired in a 12 or 6 day repeat cycle using one or both satellites, respectively, with a total coverage frequency of less than 1 day in the Arctic. This work is based on Level-1 Ground Range Detected (GRD) HH-polarized observations in Extra Wide swath mode (EW) consisting of a 400 km swath at 20x40 m spatial resolution. It uses images of both the orthorectified backscattering coefficient γ_0 and the corresponding incidence angles. Data can be downloaded from any Copernicus service, e.g. at Sentinel Hub, https://www.sentinel-hub.com/, Sinergise Ltd.

The study area is given in Figure 1 and encompasses a small area (10x20 km^2) located in the northern Barents Sea, which is considered a warming hotspots in the Arctic [7]. The region passes an entire annual cycle of freeze up, melting, and ice-free ocean and consists exclusively of first-year ice during the Arctic winter months. Figure 2 shows an example of γ_0 image in decibels (top) including its distribution and cumulative sum (bottom), acquired on April 24, 2020 at an incidence angle of 43.1 $^\circ$. The image indicates small low-valued patches which can be attributed to melt ponds.

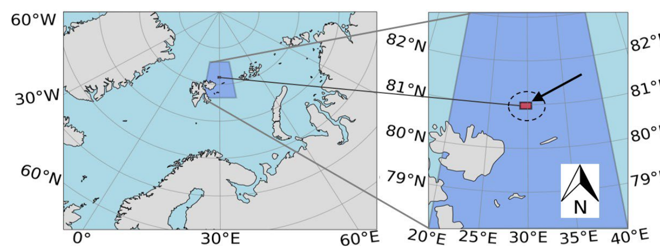

Fig. 1. Study area consisting of ~10x20 km^2 located in the northern Barents Sea between Svalbard and Franz Josef Land.

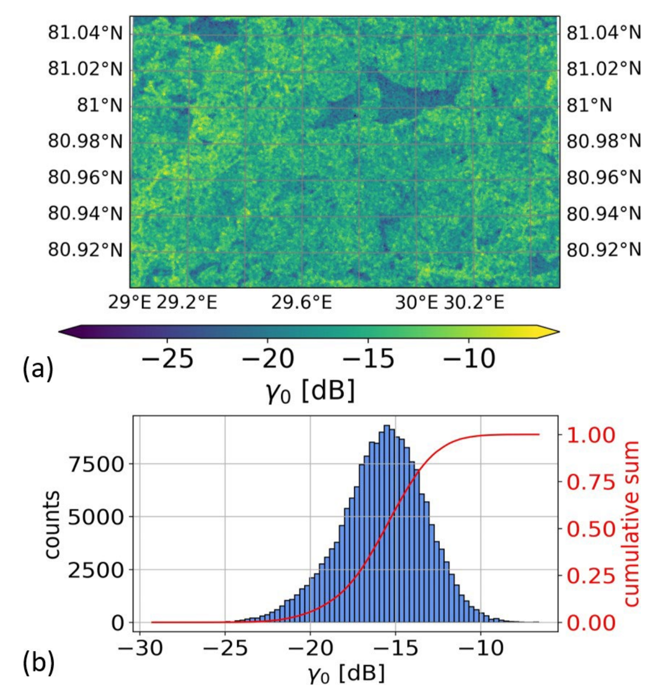

Fig. 2. Sentinel-1 backscatter coefficient γ_0 acquired on April 24, 2020, at an incidence angle of 43.1 $^\circ$. **(a)** spatial distribution of γ_0; **(b)** distribution and cumulative sum of intensities.

3. METHODOLOGY

The methodology consists of three main steps, a preceding angular normalization of the SAR images, an estimation of the number of significant classes from information criteria obtained through Expectation-Maximization, and the segmentation of the SAR images to extract the surface water fraction.

3.1. Incidence angle normalization

SAR surface signatures of Arctic sea ice depend on the incidence angle [8, 9]. The intensity of γ_0 is smaller for observations at higher angles and for smooth surfaces such as calm waters. The angular normalization of medium resolution SAR images has been considered in different approaches to detect sea ice types [10, 11, 12], but remains challenging because of high sea ice drift velocities reaching up to several kilometers per day. In this work, angular variation was determined by comparing multiple images at the days when consecutive observations collected with high angular difference were available, and values were normalized according to those obtained at a mean angle of 33 $^\circ$.

3.2. Estimation of the number of significant classes using Expectation-Maximization (EM)

EM is an unsupervised clustering method initially proposed by [13] based on an iterative process which alternates between an expectation (E) step and a maximization (M) step. It has been already applied to segment sea ice into areas of different sea ice types using multi-angular Sentinel-1 SAR images [14]. The likelihood of a Gaussian Mixture Model (GMM) under variation of the number of classes and their expected weights is maximized for the respective distributions of γ_0. The best GMM with the optimal number of classes and their corresponding weights resulting in the largest likelihood is determined using Akaike and Bayesian information criterion (AIC and BIC) [15, 16].

3.3. Bayesian segmentation of SAR images

The weight and the mean value of the class belonging to the sub-distribution of the GMM with the lowest intensities of γ_0 are extracted and compared to an approximated intensity threshold. The threshold is used to assess whether the corresponding class contains a sufficient amount of low-intense values which can be attributed to surface water and is significantly large to form a separate class in the segmentation step. A Bayesian unsupervised learning algorithm was used to segment the SAR images, which are expected to contain significant amount of surface water, according to the predefined number of classes. The framework was developed by [17] and has been applied to segment Arctic sea ice from satellite data [18]. Spatial correlations between data points are considered using Hidden Markov random fields (HMRF), and a latent field result is obtained in an iterative process based on Markov Chain Monte Carlo (MCMC) sampling. The accuracy can be determined from the misclassification rate of the final segmentation step.

4. RESULTS

Figure 3 demonstrates the EM step applied to the angular-normalized SAR image acquired on April 24, 2020. BIC and AIC scores are determined after 100 iterations while fitting the GMM to the data using 1 to 5 classes, respectively. 3 classes result in the best fit with a minimum score for both criteria. The class-specific distributions of γ_0 are separable and the weight which corresponds to the lowest mean value (21.9 %) can be considered significant to be discriminable in the segmentation. Figure 4 shows the latent field result after segmentation with 3 classes, where every pixel indicates the class with the highest class membership probability. Patches in dark blue color belong to closed water with a total weight of 10.4 %, resulting in a concentration of intact sea ice of 89.6 %. The estimated SIC is compared to a reference SIC product OSI SAF OSI-401-b in Figure 5 in the period from September 1, 2019 to August 31, 2020. The reference product is known to underestimate SIC for thin ice and due the presence of melt-pond water [1]. This is in agreement with the estimated SIC showing higher values in the beginning of the freeze-up period and during melting.

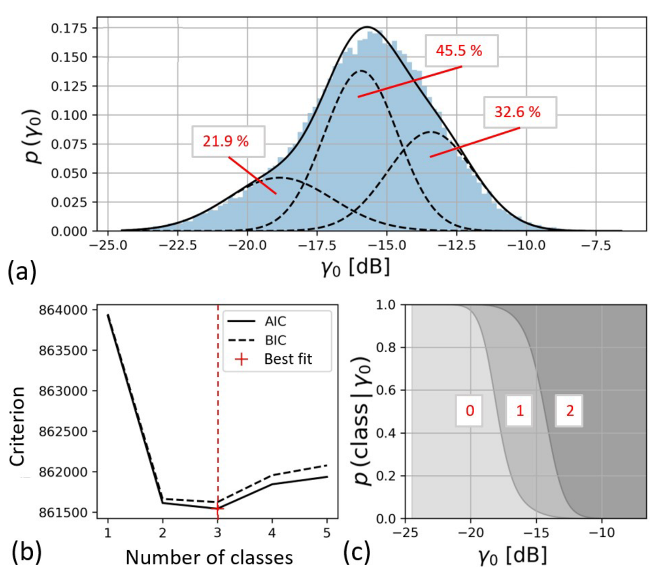

Fig. 3. EM result after 100 iterations. **(a)** Distribution of γ_0 including the weights of the best fit; **(b)** AIC and BIC scores with its minimum value obtained for an optimal number of 3 classes; **(c)** class-specific probabilities as a function of γ_0.

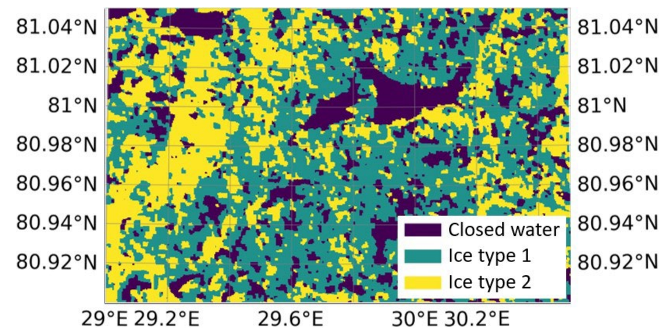

Fig. 4. Segmentation result using 3 classes to discriminate surface water fraction from sea ice types based on a SAR image acquired on April 24, 2020.

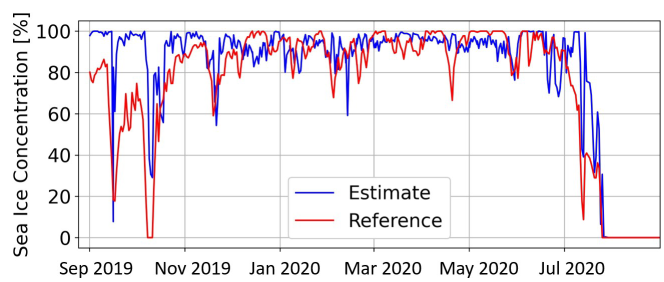

Fig. 5. Estimated concentration of intact sea ice in comparison to OSI-SAF SIC from September 1, 2019 to August 31, 2020.

5. CONCLUSION

This work proposes a probabilistic approach to segment sea ice based on Sentinel-1 SAR image to estimate the fraction of closed water including melt ponds, and the associated SIC. Aim is to combine an EM step with a Bayesian inference framework using GMM and HMRF to consider the statistical and spatial backscattering characteristics. The method was applied to an area in the northern Barents Sea and allowed to estimate SIC during an entire yearly cycle from Arctic freeze starting in September to ice-free ocean in August. The dynamics of melt ponds is governed by continuous processes and smooth transitions. Thus, unambiguous categorization through the observed SAR surface signatures is only possible when sufficient contrast is given, which limits the accuracy of any segmentation method. In future work, the probabilistic information of the model result at each pixel can be used to evaluate the uncertainty of detected surface water.

6. ACKNOWLEDGEMENTS

The lead author was supported by "la Caixa" Foundation (ID 100010434) with the fellowship code LCF/BQ/DI18/11660050, and received funding from the European Union's Horizon 2020 research and innovation programme under the Marie Sklodowska-Curie grant agreement No. 713673. The project was also funded through the award "Unidad de Excelencia María de Maeztu" MDM-2016-0600, by the Spanish Ministry of Science and Innovation through the project "L-band" ESP2017-89463-C3-2-R, and the project "Sensing with Pioneering Opportunistic Techniques (SPOT)" RTI2018-099008-B-C21/AEI/10.13039/501100011033.

7. REFERENCES

[1] Thomas Lavergne, Atle Macdonald Sørensen, Stefan Kern, Rasmus Tonboe, Dirk Notz, Signe Aaboe, Louisa Bell, Gorm Dybkjær, Steinar Eastwood, Carolina Gabarro, et al., "Version 2 of the eumetsat osi saf and esa cci sea-ice concentration climate data records," *The Cryosphere*, vol. 13, no. 1, pp. 49–78, 2019.

[2] H Eicken, HR Krouse, D Kadko, and DK Perovich, "Tracer studies of pathways and rates of meltwater transport through arctic summer sea ice," *Journal of Geophysical Research: Oceans*, vol. 107, no. C10, pp. SHE–22, 2002.

[3] E Zege, A Malinka, I Katsev, A Prikhach, Georg Heygster, L Istomina, Gerit Birnbaum, and Pascal Schwarz, "Algorithm to retrieve the melt pond fraction and the spectral albedo of arctic summer ice from satellite optical data," *Remote Sensing of Environment*, vol. 163, pp. 153–164, 2015.

[4] Yasuhiro Tanaka, Kazutaka Tateyama, Takao Kameda, and Jennifer K Hutchings, "Estimation of melt pond fraction over high-concentration arctic sea ice using amsr-e passive microwave data," *Journal of Geophysical Research: Oceans*, vol. 121, no. 9, pp. 7056–7072, 2016.

[5] Haiyan Li, William Perrie, Qun Li, and Yijun Hou, "Estimation of melt pond fractions on first year sea ice using compact polarization sar," *Journal of Geophysical Research: Oceans*, vol. 122, no. 10, pp. 8145–8166, 2017.

[6] Thomas Nagler, Helmut Rott, Markus Hetzenecker, Jan Wuite, and Pierre Potin, "The sentinel-1 mission: New opportunities for ice sheet observations," *Remote Sensing*, vol. 7, no. 7, pp. 9371–9389, 2015.

[7] Sigrid Lind, Randi B Ingvaldsen, and Tore Furevik, "Arctic warming hotspot in the northern barents sea linked to declining sea-ice import," *Nature climate change*, vol. 8, no. 7, pp. 634–639, 2018.

[8] Mallik S Mahmud, Torsten Geldsetzer, Stephen EL Howell, John J Yackel, Vishnu Nandan, and Randall K Scharien, "Incidence angle dependence of hh-polarized c-and l-band wintertime backscatter over arctic sea ice," *IEEE Transactions on Geoscience and Remote Sensing*, vol. 56, no. 11, pp. 6686–6698, 2018.

[9] Johannes Lohse, Anthony P Doulgeris, and Wolfgang Dierking, "Mapping sea-ice types from sentinel-1 considering the surface-type dependent effect of incidence angle," *Annals of Glaciology*, pp. 1–11, 2020.

[10] Marko Mäkynen and Juha Karvonen, "Incidence angle dependence of first-year sea ice backscattering coefficient in sentinel-1 sar imagery over the kara sea," *IEEE Transactions on Geoscience and Remote Sensing*, vol. 55, no. 11, pp. 6170–6181, 2017.

[11] Alexander S Komarov and Mark Buehner, "Detection of first-year and multi-year sea ice from dual-polarization sar images under cold conditions," *IEEE Transactions on Geoscience and Remote Sensing*, vol. 57, no. 11, pp. 9109–9123, 2019.

[12] Anca Cristea, Jeroen van Houtte, and Anthony P Doulgeris, "Integrating incidence angle dependencies into the clustering-based segmentation of sar images," *IEEE Journal of Selected Topics in Applied Earth Observations and Remote Sensing*, vol. 13, pp. 2925–2939, 2020.

[13] Arthur P Dempster, Nan M Laird, and Donald B Rubin, "Maximum likelihood from incomplete data via the em algorithm," *Journal of the Royal Statistical Society: Series B (Methodological)*, vol. 39, no. 1, pp. 1–22, 1977.

[14] Ronny Hänsch, Joel Alfredo Amao Oliva, Ralf Horn, Marc Jäger, and Rolf Scheiber, "Unsupervised clustering of c-band polsar data over sea ice," 2020.

[15] Hirotugu Akaike, "A new look at the statistical model identification," *IEEE transactions on automatic control*, vol. 19, no. 6, pp. 716–723, 1974.

[16] Gideon Schwarz et al., "Estimating the dimension of a model," *The annals of statistics*, vol. 6, no. 2, pp. 461–464, 1978.

[17] Hui Wang, J Florian Wellmann, Zhao Li, Xiangrong Wang, and Robert Y Liang, "A segmentation approach for stochastic geological modeling using hidden markov random fields," *Mathematical Geosciences*, vol. 49, no. 2, pp. 145–177, 2017.

[18] Christoph Herbert, Adriano Camps, Florian Wellmann, and Mercedes Vall-llossera, "Bayesian unsupervised machine learning approach to segment arctic sea ice using smos data," *Geophysical Research Letters*, vol. 48, no. 6, pp. e2020GL091285, 2021.